

Time-frequency analysis of visual evoked potentials for interhemispheric transfer time and proportion in callosal fibers of different diameters

Ilkay Ulusoy¹, Ugur Halici¹, Erhan Nalçacı², Ilker Anaç¹, Kemal Leblebicioğlu¹, Canan Başar-Eroğlu³

¹ Department of Electrical and Electronics Engineering, Computer Vision and Intelligent Systems Research Laboratory, Middle East Tech. U., 06531, Ankara, Turkey

² Physiology Department, Cognitive Neurophysiology Unit, Ankara University, School of Medicine, Ankara, Turkey

³ Psychology and Cognitive Research Institute, Bremen University, Bremen, Germany

Received: 24 March 2003 / Accepted: 28 January 2004 / Published online: 6 April 2004

Abstract. This study is an extension of the experimental research of Nalçacı et al., who presented 16 subjects with a reversal of checkerboard pattern as stimuli in the right visual field or left visual field and recorded EEG at O1, O2, P3, and P4. They applied the chosen bandpass filters (4–8, 8–15, 15–20, 20–32 Hz) to the VEPs of subjects and obtained four different components for each VEP. The first aim of this study is to improve the previous report using some methods in time-frequency domain to estimate interhemispheric delays and amplitudes in a time window. Using the improved estimates of interhemispheric delays, the second aim is to estimate the proportion of callosal fibers of different diameters that are activated by visual stimuli by comparing amplitudes of VEPs in different frequency bands. If the relation between frequency components of VEP and delays for callosal fibers of different dimension were reliable, it would give us an opportunity to deal with amplitude of bandpass-filtered VEPs in order to see approximately the proportion of these fibers activated by a certain stimulus. By using frequency-dependent shifts in time and maximizing the cross correlation of direct VEP (DVEP–VEP obtained from contralateral hemisphere)–indirect VEP (IVEP–VEP obtained from ipsilateral hemisphere) pairs in the time-frequency domain, we examined the delay not only at P100 and N160 peaks but along a meaningful time interval as well. Furthermore, by shifting back the IVEP according to the delay estimated at each time window, both the amplitudes and energies of the synchronized DVEP–IVEP pairs were compared at the chosen frequency bands. The percentages of IVEPs at each band was then examined further in conjunction with the distribution of axon diameters in the posterior pole of the CC, questioning the relation between the distributions of the axon diameters and activations at each band. We established an energy

definition to express the activation in the fibers. When the energy percentages of IVEPs in theta and alpha were totaled, they were found to be between 76.2% and 81.6%, which is close to the value 74–77% for fibers of 0.4–1 μm in diameter obtained from anatomical study of human CC. The sum of energy percentages in the beta1 and beta2 bands was between 20.1% and 24.2%, which probably reflects the proportion of activation of callosal fibers 1–3 μm in diameter.

Abbreviations: CC corpus callosum – DVEP direct VEP – EEG electroencephalogram – EOG electrooculogram – IHTT interhemispheric transfer time – IVEP indirect VEP – LVF left visual field – RT reaction time – RVF right visual field – VEP visually evoked potential

1 Introduction

The brain is composed of two hemispheres, each being functionally specialized for certain cognitive processes. Besides some subcortical connections between hemispheres, the corpus callosum (CC), as the largest fiber tract in the brain, seems to have the greatest responsibility for the integration of hemispheric functions (Gazzaniga 2000). On the other hand, Nowak and Bullier (1997) suggested that the functions of the brain could be explained by the fast and the slow brain models. The fast analysis system appears to be devoted to the processing of localization and visuomotor integrations, while the slow processing system deals with fine detail analysis and precise recognition. As the largest fiber tract, the CC should also have slow and fast conducting systems, but not a homogenic system.

In fact, studies reveal that conduction times vary within a large range. Swadlow (1974) studied conduction time in the callosal pathway of rabbits using electrical stimulation and showed that the shortest antidromic

Correspondence to: I. Ulusoy
(e-mail: ilkay@metu.edu.tr,
Tel.: +90-312-2104558, Fax: +90-312-2101261)

latency was 2.4 ms, but most latencies were long, with a maximum value of 38.9 ms. Conduction times in cat callosal axons also show this variety, even though the shorter conduction time was measured in comparison to that of the rabbit (Innocenti et al. 1995). These findings are consistent with anatomical studies that revealed huge variation in axonal diameters (for review, see Hoptman and Davidson 1994), and conduction velocity and axon diameter are linearly related (Waxman and Bennett 1972). All regions of the CC have a preponderance of small fibers, but they vary in the proportion of myelinated axons and larger fibers. Aboitiz et al. (1992), who performed a light microscopic examination in the CC of human brains, have divided the CC into ten segments and characterized the different callosal segments in terms of the densities of fibers of different size. The myelinated fibers of the CC are grouped into four according to their diameter such as fibers greater than 0.4, 1, 3, and 5 μm in diameter. While sensory areas tend to be connected through large-diameter myelinated fibers, higher-order processing areas tend to be connected through small-diameter, lightly myelinated fibers (Aboitiz et al. 1992). This suggests that the CC has different types of channels, relating to the kind of information transferred from one hemisphere to the other (Clarke and Zaidel 1994).

Many studies have been performed to estimate interhemispheric transfer time (IHTT) in the human brain. Initially, the estimate of IHTT was based on the comparison of manual reaction times (RT) for stimuli presented briefly to the ipsilateral or contralateral visual hemifield of the response hand. IHTTs of young healthy people were found to be in the range of 2–6 ms by many researchers using simple RT (for review, see Bashore 1981). However, this result was found to be contrary to anatomical evidences, as this speed is too fast for the majority of callosal fibers (Davidson and Saron 1992; Hoptman and Davidson 1994). Transfer time at this speed requires large ($> 2.4 \mu\text{m}$), myelinated fibers, and Aboitiz et al. (1992) found that this kind of fiber is relatively rare.

Other researchers have used visual evoked potentials (VEPs) to estimate IHTT (Rugg et al. 1984; Brown and Jeeves 1993). In this method, VEPs with lateralized brief stimuli have been recorded from homologous sites on the scalp of human subjects. Time-locked waveforms, particularly P100 and N160, have been used to estimate IHTT, measuring the difference in latency between ipsilateral (IVEP) and contralateral (DVEP) sites. The term “Direct VEP (DVEP)” is used here to represent the VEP produced in the contralateral visual hemifield, and “Indirect VEP (IVEP)” is used for the VEP produced in the other hemisphere, mostly via the CC. VEP studies yielded longer estimates of IHTT. Saron and Davidson (1989) estimated IHTT using VEPs to lateralized checkerboard flashes presented in a simple RT task and found it to be approximately 12 ms between peaks obtained from the occipital cortex.

Nalçacı et al. (1999a) recently suggested that, even though different estimations of IHTT have been found depending on the type of paradigms and the measuring

sites, only a latency difference has been measured between two peaks of complex waves in each VEP study. However, these complex waves of VEP were most probably formed by different generators of neural populations that act through different frequency channels (Başar 1988). The slow and fast components of VEPs are entirely generated in cortical layers (Ducati et al. 1988). Nalaaci et al. (1999a) hypothesized that if the main peaks of VEP were established by different types of generators, which can also be connected to each other by different types of callosal fibers, a wide range IHTT could be estimated by measuring the latency between time-locked peaks of narrow bandpass-filtered VEP.

Nalçacı et al. (1999a,b) carried out an experiment to test this hypothesis, and subjects were presented with a reversal of a checkerboard pattern as stimuli at right visual field (RVF) or left visual field (LVF), and EEG was recorded at O1, O2, P3, and P4. The grand-averaged VEPs were transformed to the frequency domain by means of the fast Fourier transform to obtain the amplitude frequency characteristics. Bandpass filters were chosen appropriately according to tuning frequencies indicated by clear peaks in the amplitude frequency characteristics. The chosen bandpass filters [4–8 Hz (θ), 8–15 Hz (α), 15–20 Hz (β_1), 20–32 Hz (β_2)] were applied to the VEP of the subjects, and four different components of VEPs for each VEP were obtained. The latency of P100 and N160 of unfiltered VEP was measured. By means of the bandpass filters applied to VEPs, positive and negative peaks consistent with P100 and N160 were measured for each subject. The P100 latency was defined as the latency of the greatest positivity between 80 and 130 ms. The N160 latency was defined as the latency of the greatest negativity between 130 and 190 ms. In the 20–32 Hz band, the largest amplitudes of negative and positive peaks were observed between 70 and 120 ms. The first high negative peak was defined as N80, and the first high positive peak was defined as P100. These peaks were selected for evaluation. Latency differences between hemispheres for digitally unfiltered and filtered VEPs were computed to estimate IHTT. In the different frequency bands, different IHTTs were estimated, ranging from 3 to 30 ms. Approximately 16 ms for θ band, 11 ms for α band, 6 ms for β_1 band, and 3 ms for β_2 band were found.

This study is an extension of the experimental research of Nalçacı et al. (1999a,b). All previous reports that have attempted to estimate VEP–IHTT depended on the latency difference between main peaks of VEP. However, peaks reflect only one moment of neural activation and data are lost unless evaluation of whole VEP waves in a time window is carried out. First, this study aims to improve the previous report using some methods in time-frequency domain to estimate interhemispheric delays and amplitudes in a time window.

In addition, this study aims to estimate the percentage of callosal fibers of different diameters activated by visual stimuli by comparing amplitudes of VEPs at different frequency bands. Frequency–amplitude analysis of VEP for IHTT was first carried out in the reports of Nalçacı et al. (1999a,b). However, to date there is no

study on IHTT-VEP dealing with the amplitude of direct and indirect VEPs. If the relation between the frequency component of VEP and delays for callosal fibers in different dimensions were reliable, it would give us an opportunity to deal with amplitude of bandpass-filtered VEPs to see approximately the proportion of these fibers activated by a certain stimulus.

2 Materials and methods

2.1 Data

In this study, VEP pairs (i.e., pairs of DVEP and IVEP) from the same experimental data set of Nalçacı et al. (1999b), in which right-handed men ($n=8$) and women ($n=8$) between the ages of 19 and 30 years served as subjects, were used. The stimuli reversals of a 55' checkerboard pattern were presented as a window $8.5 \times 8.5 \text{ cm}^2$. The medial edge of the stimulus was 2° to the left or right of the central point. Nalçacı et al. (1999b) carried out two different blocks of experiments in the following way: stimuli were presented to the right visual hemifield (RVF) or the left visual hemifield (LVF). In each block, 120 stimuli were presented and 120 trials results collected. Interstimulus intervals varied randomly between 2.5 and 3.5 s.

EEG was recorded with Ag/AgCl electrodes positioned at O1, O2, P3, and P4 according to the 10/20 systems. The linked ear lobes (A1 + A2) served as reference. Two channels of EOG were recorded from electrodes placed on the outer canthus of the right eye and above the right eyebrow to measure horizontal and vertical eye movements. Electrode impedances were below 5 k Ω . EEGs were amplified by a Nihon Kohden (EEG-4421) EEG apparatus with band limits 0.1–70 Hz (24 dB/octave). An additional 50-Hz notch filter was also applied to the data to remove main interference. EEG records began 1 s prior to stimulus onset and extended 1 s poststimulus. Each channel was digitized on line with a sampling rate of 500 samples per second and stored on computer disc for later averaging.

With respect to EOG amplitude, any EEG trials associated with artifacts were automatically rejected. In addition to this rejection procedure, single sweep analysis was carried out on each EOG channel, and EEG trials associated with blink and saccadic eye movements were eliminated before averaging.

In our analysis of the VEPs obtained by Nalçacı et al. (1999b), the parts corresponding to the interval [0–1] s just after the stimuli were used.

2.1 Delay calculation

DVEPs and IVEPs were separated into θ , α , β_1 , and β_2 bands using bandpass filters. For determining the interhemispheric delay for each band, the cross correlation $C(\text{DVEP}, \text{IVEP})$ of the filtered DVEP, IVEP pairs was considered. Let Δ_b be the window size at band $b = \theta, \alpha, \beta_1, \beta_2$ to be used in correlation

calculation. In this study, it was chosen as $\Delta_\theta = 128 \text{ ms}$, $\Delta_\alpha = 64 \text{ ms}$, $\Delta_{\beta_1} = 32 \text{ ms}$, $\Delta_{\beta_2} = 16 \text{ ms}$ such that it covered at least one cycle of the signal. Let $\text{DVEP}_b [s, \Delta_b]$ represent the portion of the DVEP at the chosen band b , containing $\Delta_b/2$ sample points (since sampled at 500 Hz) starting from s . Similarly, let $\text{IVEP}_b [s, \Delta_b]$ represent IVEP. The interhemispheric transfer may not begin before 50 ms, and the transfer is almost completed after 200 ms. Since the correlation of VEP pairs was observed to be low before $s < 50$ and after $s > 200$ ms, we restricted this to $50 \text{ ms} \leq s \leq 200 \text{ ms}$. For each data point k in interval [50 ms, 200 ms] we determined delay d_{k_b} such that the cross correlation $C(\text{DVEP}_b [k, \Delta_b], \text{IVEP}_b [k+d_{k_b}, \Delta_b])$ was maximum (1, 2). In Eq. (2) m_{DVEP_b} and m_{IVEP_b} are the mean of the DVEP and IVEP in the restricted range:

$$d_{k_b} = \arg \max_d C(\text{DVEP}_b [k, \Delta_b], \text{IVEP}_b [k+d, \Delta_b]) \quad (1)$$

$$C(\text{DVEP}_b [k, \Delta_b], \text{IVEP}_b [k+d, \Delta_b]) = \int_k^{k+\Delta_b} (\text{DVEP}_b(t) - m_{\text{DVEP}_b})(\text{IVEP}_b(t+d) - m_{\text{IVEP}_b}) dt. \quad (2)$$

In this way, delay values were determined not only at peak points such as P100 or N160 but for all points in the interval from 50 to 200 ms. In Fig. 1a, DVEP and IVEP in the theta band of a good sample of the subjects were plotted. In Fig. 1b, the delay values found for each time were plotted. As can be observed from the figures, IVEP is later and smaller than DVEP.

Furthermore, we considered the normalized (Pearson) correlation of VEPs as a whole, i.e., $C(\text{DVEP}_b [50, 150], \text{IVEP}_b [50+d, 150])$, to determine a single delay

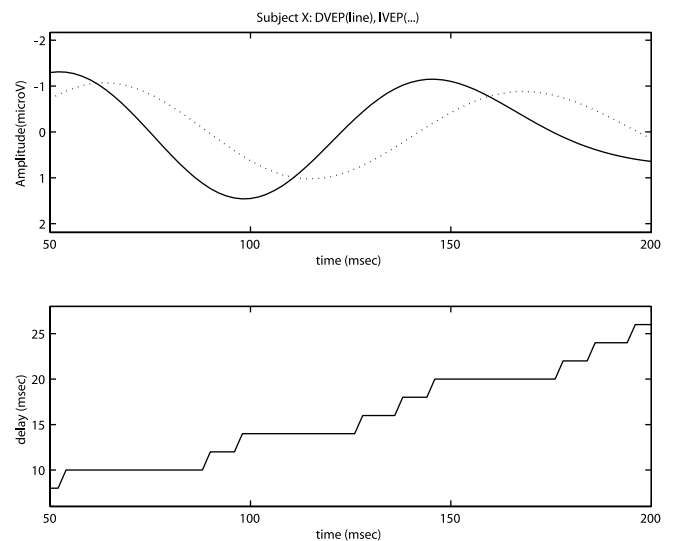


Fig. 1. **a** Amplitudes (V) of a subject's DVEP (—) and IVEP (...) in the theta band (*upper graph*). **b** Delay (ms) between the DVEP and IVEP at each time point (*lower graph*)

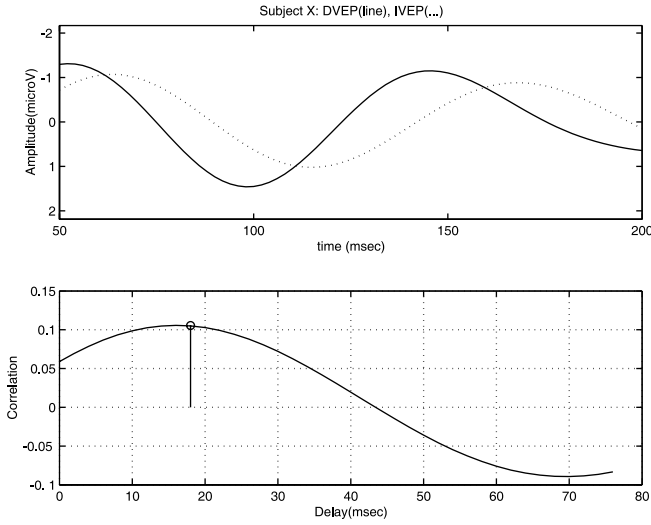


Fig. 2. **a** Amplitudes (V) of a subject's DVEP (—) and IVEP (...) in the theta band (*upper graph*). **b** Time series of Pearson correlation coefficients (*lower graph*). The delay for which correlation is maximum is marked on the plot

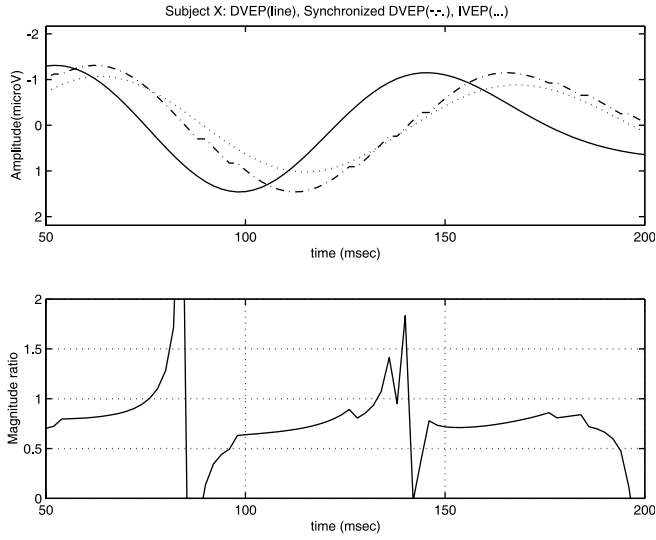


Fig. 3. **a** Amplitudes (V) of a subject's DVEP (—), IVEP (...), and synchronized DVEP (-.-.-) in the theta band (*upper graph*). **b** Magnitude ratio for IVEP and synchronized DVEP (*lower graph*)

value d_b for each band. DVEP and IVEP in the theta band are given in Fig. 2a. The correlation results and the delay values are given in Fig. 2b.

In the next step of our analysis, we compared the magnitudes of DVEP and IVEP signals. For this purpose, we synchronized DVEP_b and IVEP_b by shifting DVEP_b forward according to d_{k_b} values estimated at each k in the chosen band b and then compared the amplitudes of DVEP_b and IVEP_b at peak points. In Fig. 3a, DVEP, IVEP, and synchronized DVEP in the theta band are shown in the top image with the delay found for each time (i.e., d_{k_0}). The amplitude ratio of the synchronized DVEP and the IVEP is given in Fig. 3b. The amplitudes are taken with respect to zero.

2.3 CC model and estimate of fiber percentage in different dimension

The energy in a narrow interval around P100 of IVEP_b gives some idea about how much of the signal is transferred through the CC at each band. This energy information is used to estimate the ratio of different fiber types that were effective during the information transfer of the stimulus from the contralateral hemisphere to the other hemisphere. For this purpose we used a very simple model of the callosal transfer in the CC as given in Fig. 4. In this figure, besides our CC model, a simple drawing for visual processing in the brain when the stimulus is provided from the RVF is given. Here, the right and left hemispheres are shown as large rectangles. The information is carried from the retina through the lateral geniculate nucleus (LGN) up to the visual cortex through parallel pathways. The total effect of the parallel pathways can be modeled in the same manner as our CC model. The activations of the neuron populations are obtained by EEG sensors, which are shown as small rectangles and modeled with the function f in the figure. Thus, VEPs obtained from the scalp are the neuronal activities passed through this unknown filter f , which is the same for both sites and is assumed to be linear. Lines connecting the hemisphere rectangles show the channels in the CC structure. Each channel is supposed to carry a specific frequency band of information (i.e., $\theta, \alpha, \beta 1, \beta 2$) and is modeled to have n_b number of fibers of a type, $b = \{\theta, \alpha, \beta 1, \beta 2\}$, where $k_b(t)$ percent of n_b fibers is active at any time of the transfer duration. Each fiber in a channel is assumed to create a potential of v_b at the end on average and this value is assumed to be the same for all fibers irrespective of the type. In calculating energy, a small interval around P100 is considered and based on the information that at P100 as many fibers as possible are active. Since the signal is almost flat around peak value, $k_b(t)$ is supposed to be the same for all times in this small interval and also the same for all channels.

According to the model, IVEP can be calculated as follows:

$$\text{IVEP}(t) = f \left(\sum_{b=\{\theta, \alpha, \beta 1, \beta 2\}} n_b v_b k_b(t) \right). \quad (3)$$

Using the assumption that f is linear, i.e., $f(x) = \kappa x$,

$$\text{IVEP}(t) = \sum_{b=\{\theta, \alpha, \beta 1, \beta 2\}} \kappa n_b v_b k_b(t) = \sum_{b=\{\theta, \alpha, \beta 1, \beta 2\}} m_b(t), \quad (4)$$

where $m_b(t) = \kappa n_b v_b k_b(t)$.

The normalized root energy for a band b around P100 is calculated as follows:

$$E_b = \sqrt{\frac{\int_{I_b} (m_b(t))^2 dt}{|I_b|}}$$

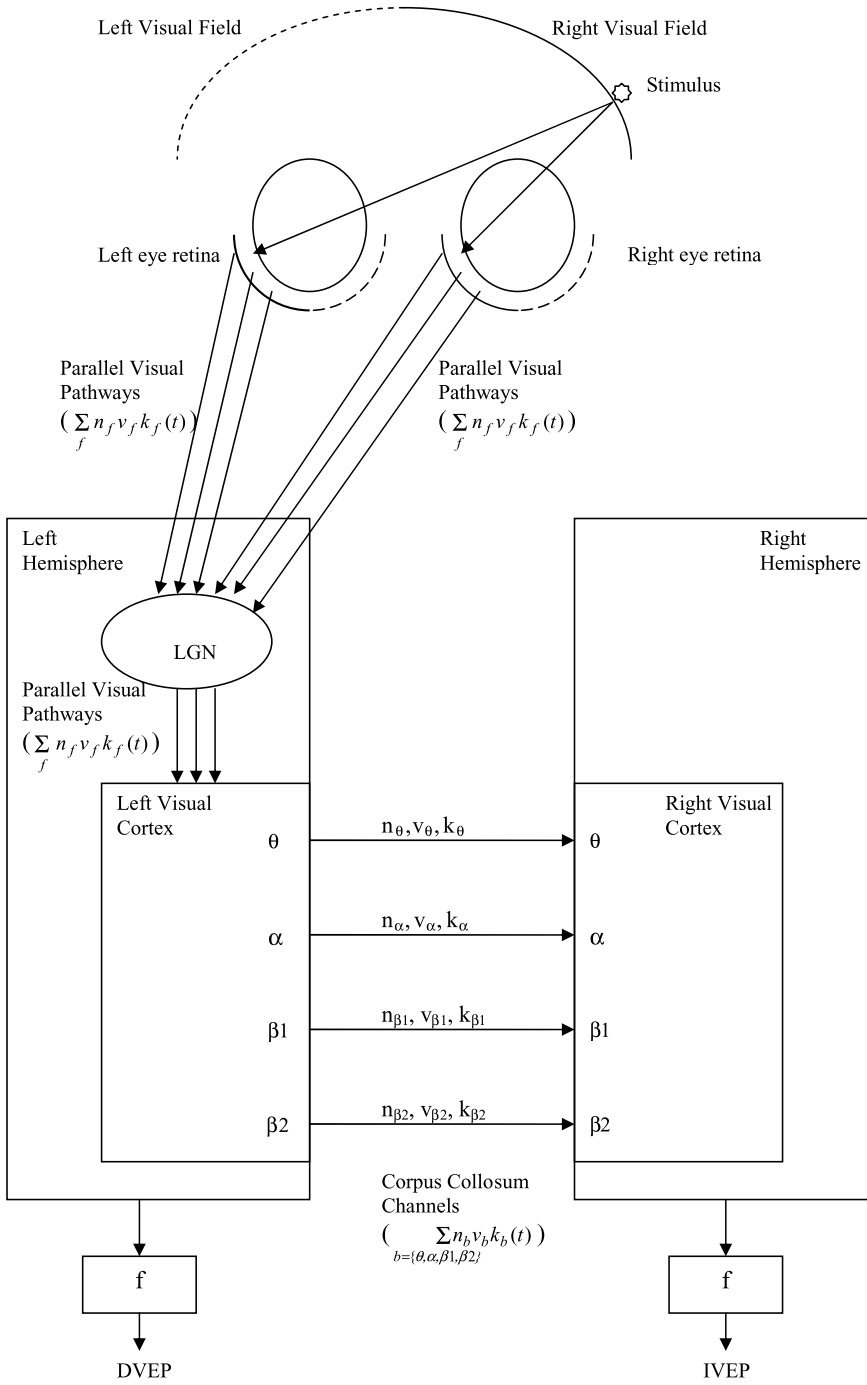


Fig. 4. A simple drawing for visual processing in the brain and our CC model. In this case stimulus is provided from RVF. The information is carried from the retina through the LGN up to the visual cortex through parallel pathways. The total effect of the parallel pathways can be modeled by $\sum_f n_f v_f k_f(t)$ in the same manner as our CC model, where f defines different fiber types carrying information at different frequencies. CC channels $b = (\theta, \alpha, \beta_1, \beta_2)$ connect the hemispheres, where n_b is the number of fibers of a type in channel b , k_b is the percent of active fibers, and v_b is the potential created by a fiber in channel b

$$\begin{aligned}
 &= \sqrt{\frac{\int_{I_b} (\kappa n_b v_b k_b(t))^2 dt}{|I_b|}} \\
 &= \sqrt{\frac{\kappa^2 n_b^2 v_b^2}{|I_b|} \int_{I_b} k_b(t)^2 dt}, \quad (5)
 \end{aligned}$$

where I_b is the interval around P100 in band $b = \{\theta, \alpha, \beta_1, \beta_2\}$ in order to calculate the energy and $|I_b|$ is the length of the interval that is chosen to be one eighth of the wavelength of the highest frequency. Using

the assumption that k_b is constant in the interval I_b and is also the same for all b , we can write

$$E_b = \sqrt{\frac{\kappa^2 n_b^2 v_b^2 k^2 |I_b|}{|I_b|}}, \quad (6)$$

where k is the constant value of $k_b(t)$ during the interval. Using the assumption that v_b is the same for all channels, the energy for band b becomes

$$E_b = \sqrt{\kappa^2 v^2 k^2 n_b^2} = \kappa v k n_b = C n_b, \quad (7)$$

where $C = \kappa v k$.

The total energy is the sum of the energy over the bands and is the energy of the IVEP in the interval I_b around P100:

$$E = \sum_{b=\{\theta,\alpha,\beta1,\beta2\}} Cn_b = C \sum_{b=\{\theta,\alpha,\beta1,\beta2\}} n_b . \quad (8)$$

If we calculate the ratio of a band energy over the whole energy, it becomes

$$R_b = \frac{E_b}{E} = \frac{n_b}{\sum_{b=\{\theta,\alpha,\beta1,\beta2\}} n_b} . \quad (9)$$

Thus, with our assumptions, this energy ratio gives us an estimate of the ratio of a fiber type to all fibers. We can say that the number of fibers in channel b is R_b percent of the total number of fibers used in the transfer.

2.4 Statistical analysis

To estimate the mean ratio of callosal fibers across 16 subjects, we eliminated some of the subjects whose delays were found to be in an unexpected direction in a time window for the RVF or LVF experiment. IHTT in the expected direction can be defined as a condition where IVEP occurs later than DVEP. Therefore, we computed the estimate of fiber ratio when the callosal transfer was realized in all the given frequency channels. Differences among four frequency bands for the delays, magnitudes, and energies were evaluated by Friedman two-way analysis of variance by ranks. Amplitudes and energies of DVEP and IVEP were also compared using the Wilcoxon signed ranks test.

3 Results

3.1 Delays between the hemispheres

The average values of VEPs obtained at the occipital and the parietal sites are summarized in Tables 1 and 2, respectively. The results are consistent with previous reports (Nalçacı et al. (1999a,b)). The longest delays between the hemispheres belonged to the theta band, indicating that the slowest conductance was found to be in this frequency band. The delays in this frequency band varied between 15.75 and 21.64 ms. Instead of peak evaluation, estimate of interhemispheric transfer time in a whole signal yielded a longer estimate for the theta band (around 20 ms). The delays in the alpha frequency band varied between 7.00 and 16.75 ms, indicating faster conductance than in the theta band. Delays in the beta1 band were measured as 5.75–11.33 ms. In the beta2 band, the highest velocity was found to be 0.73–4.73 ms. The measurement of delays in a whole signal at the beta2 band seems to be more reliable, varying between 3.25 and 4.73 ms.

This different estimate of IHTTs supports the hypothesis that depends on a linear relation between firing frequency of oscillatory neurons and dimension of

fibers for callosal transfer. Long delays suggest that there are neurons of a generator that fire at slow frequency and have small axons, and vice versa.

3.2 Magnitudes and energies

Some magnitudes and energy differences between DVEP and IVEP were found to be statistically significant for frequency bands in different conditions of the experiments (Tables 1 and 2). In general, magnitudes and energies of IVEP were smaller than those of DVEP probably due to filtration of information during hemispheric transfer.

As magnitudes of IVEP showed negative correlation with frequency bands, the measurement of VEP magnitudes in the different frequency bands also supports the main theme of this study (Tables 1 and 2). DVEP magnitudes and energies show the same type of behavior as IVEP. The largest magnitudes were obtained in the theta band in which small and thinly myelinated fibers might be responsible for callosal transfer. The major component of the CC consists of small and thinly myelinated fibers; therefore our results are consistent with anatomical findings. On the other hand, larger fibers of the CC making up a small portion of the CC oscillate at high frequency, and the smallest magnitude was measured for the beta2 band.

The values of magnitude percentage for IVEP were obtained as 31.06–41.38% for the theta band, 39.0–42.0% for the alpha band, 12.0–16.93% for the beta1 band, and 8.84–11.44% for the beta2 band. Even though the results of energy percentage for IVEP were in parallel with those of magnitude percentage, the values obtained from energies seem to be more coherent, considering the negative correlation between speed of frequency and proportion of fibers of different dimensions. The values of energy percentage were 34.82–46.72% for the theta band, 33.72–41.39% for the alpha band, 10.42–14.53% for the beta1 band, and 6.56–9.63% for the beta2 band. These percentages could reflect the percentage of callosal fibers of different diameters that were activated by visual stimuli in the posterior part of the CC.

4 Discussion

In the postmortem study of the human brain, Aboitiz et al. (1992) investigated fiber composition of the CC using light microscopic examination. They calculated delays between the hemispheres using anatomical data, and it was assumed that there was a linear relation between fiber diameter and velocity. The distance between visual areas in the hemispheres are known to range from 100 to 130 mm. Dividing the distance of the estimated velocity for each fiber, delay values can be calculated. For unmyelinated fibers, delay values were found in a range of 50 to 433 ms. For myelinated fibers of different diameters, delay values were as follows: for fibers 0.4 μm in diameter between 19.2 and 24.9 ms, for fibers 1 μm in diameter between 7.6 and 9.9 ms, for fibers 3 μm in

Table 1. Mean values and standard deviations of delays, magnitudes, and energies of DVEP and IVEP for each frequency band for LVF and RVF experiments at the occipital site

Frequency band	Delay for P100 (ms)	Delay for negative peaks (ms)	Delay for whole signal (ms)	Magnitude of DVEP (V)	Magnitude of IVEP (V)	Magnitude of IVEP (%)	p values (Wilcoxon test between DVEP and IVEP Magnitude)	Magnitude percentage for IVEP (%)	Energy of DVEP	Energy of IVEP	p values (Wilcoxon test between DVEP and IVEP energy)	Energy percentage for IVEP, R_b (%)
LVF ($n = 11$)												
theta (θ)	16.36 ± 18.44	17.64 ± 20.92	21.64 ± 16.05	0.79 ± 0.61	0.43 ± 0.42	31.06 ± 23.83	<0.05	13.75 ± 17.0	5.07 ± 9.14	5.07 ± 9.14	<0.05	34.82 ± 24.42
alpha (α)	10.0 ± 6.63	11.27 ± 8.78	10.00 ± 7.10	0.73 ± 0.51	0.56 ± 0.34	42.5 ± 18.71	n.s.	7.08 ± 8.46	3.69 ± 4.20	3.69 ± 4.20	n.s.	41.39 ± 18.63
beta1 (β_1)	8.91 ± 6.09	8.73 ± 5.46	8.73 ± 6.15	0.31 ± 0.16	0.20 ± 0.12	16.93 ± 9.82	<0.05	0.75 ± 0.67	0.39 ± 0.41	0.39 ± 0.41	<0.05	14.53 ± 8.08
beta2 (β_2)	3.82 ± 5.62	0.73 ± 4.92	4.73 ± 5.46	0.25 ± 0.19	0.12 ± 0.07	9.27 ± 5.46	<0.05	0.39 ± 0.55	0.17 ± 0.16	0.17 ± 0.16	n.s.	9.63 ± 5.46
p values (Friedman)	n.s.	<0.05	<0.05	<0.0001	<0.0001	<0.0001						
RVF ($n = 8$)												
theta (θ)	17.00 ± 14.89	15.75 ± 15.29	21.25 ± 15.08	0.93 ± 0.49	0.77 ± 0.55	41.38 ± 18.25	n.s.	15.22 ± 12.72	12.29 ± 15.20	12.29 ± 15.20	n.s.	46.72 ± 18.98
alpha (α)	9.00 ± 9.68	7.00 ± 10.9	9.00 ± 9.86	1.21 ± 0.77	0.82 ± 0.90	34.85 ± 23.34	n.s.	17.73 ± 18.68	13.21 ± 18.02	13.21 ± 18.02	n.s.	33.72 ± 22.60
beta1 (β_1)	6.89 ± 5.21	8.00 ± 5.13	7.50 ± 3.69	0.26 ± 0.14	0.22 ± 0.15	12.32 ± 6.03	n.s.	0.58 ± 0.47	0.49 ± 0.50	0.49 ± 0.50	n.s.	10.42 ± 5.15
beta2 (β_2)	1.25 ± 6.04	-2.5 ± 3.16	3.25 ± 7.63	0.24 ± 0.17	0.16 ± 0.15	11.45 ± 7.92	<0.05	0.36 ± 0.43	0.35 ± 0.48	0.35 ± 0.48	n.s.	9.63 ± 6.65
p values (Friedman)	<0.05	<0.0001	<0.0001	<0.0001	<0.0001	<0.0001					<0.0001	

Table 2. Mean values and standard deviations of delays, magnitudes, and energies of DVEP and IVEP for each frequency band for LVF and RVF experiments at the parietal site

Frequency band	Delay for P100 (ms)	Delay for negative peaks (ms)	Delay for whole signal (ms)	Magnitude of DVEP (V)	Magnitude of IVEP (V)	Magnitude (V)	p values (Wilcoxon test between DVEP and IVEP Magnitude)	Magnitude percentage for IVEP (%)	Energy of DVEP	Energy of IVEP	p values (Wilcoxon test between DVEP and IVEP energy)	Energy percentage for IVEP, R_b (%)	
LVF ($n = 6$)	theta (θ)	17.0 ± 23.21	19.0 ± 22.65	21.33 ± 16.28	0.75 ± 0.40	0.51 ± 0.29	<0.05	38.89 ± 18.62	10.20 ± 10.05	4.31 ± 2.71	<0.05	38.89 ± 18.62	
	alpha (α)	10.0 ± 12.20	8.33 ± 13.23	11.00 ± 15.32	0.92 ± 0.55	0.61 ± 0.41	<0.05	40.39 ± 16.15	10.04 ± 11.95	5.06 ± 6.95	<0.05	38.49 ± 13.53	
	beta1 (β_1)	11.33 ± 9.27	10.67 ± 8.82	11.00 ± 8.37	0.27 ± 0.13	0.22 ± 0.10	n.s.	16.11 ± 8.44	0.58 ± 0.50	0.43 ± 0.29	n.s.	13.32 ± 6.96	
	beta2 (β_2)	3.33 ± 5.75	2.33 ± 4.80	4.33 ± 4.27	0.19 ± 0.14	0.12 ± 0.06	n.s.	9.00 ± 5.00	0.21 ± 0.28	0.25 ± 0.25	n.s.	9.30 ± 6.24	
	p values (Friedman)	n.s.	n.s.	<0.05	<0.0001	<0.05	<0.05	n.s.	<0.0001	<0.05	<0.05	<0.05	<0.05
	RVF ($n = 8$)	theta (θ)	17.25 ± 11.41	15.50 ± 12.64	20.25 ± 10.93	0.85 ± 0.43	0.78 ± 0.52	n.s.	38.31 ± 17.31	12.36 ± 10.83	11.88 ± 13.99	n.s.	43.38 ± 18.06
		alpha (α)	15.75 ± 11.88	12.75 ± 13.9	16.75 ± 15.08	1.17 ± 0.83	0.78 ± 0.77	<0.05	39.00 ± 23.18	17.83 ± 29.33	10.59 ± 20.29	<0.05	38.17 ± 23.14
		beta1 (β_1)	5.75 ± 4.06	6.50 ± 4.63	5.75 ± 4.59	0.21 ± 0.10	0.26 ± 0.14	n.s.	13.85 ± 7.54	0.34 ± 0.25	0.63 ± 0.57	<0.05	11.88 ± 5.45
		Beta1 (β_2)	-1.25 ± 3.69	2.00 ± 5.76	4.50 ± 8.12	0.25 ± 0.18	0.22 ± 0.26	n.s.	8.84 ± 5.39	0.38 ± 0.54	0.27 ± 0.46	n.s.	6.56 ± 4.45
		P values (Friedman)	<0.0001	<0.05	<0.0001	<0.0001	<0.0001	<0.0001	n.s.	<0.0001	<0.0001	<0.0001	<0.0001

diameter between 2.5 and 3.2 ms, and for fibers 5 μm in diameter between 1.5 and 1.9 ms. Our results were obtained from the living human brain, and a comparison with anatomical data makes it possible to conclude that delays in the theta band are related to transfer through fibers around 0.4 μm in diameter. Delays in the alpha band seem to be related to callosal transfer through fibers around 0.4–1 μm in diameter. Delays in the beta1 band could be related to callosal transfer through fibers around 1 μm in diameter, and delays in the beta2 band could also be correlated with interhemispheric transfer through fibers around 3 μm in diameter. When we compare the results of these two anatomical and electrophysiologically based experiments, it could be claimed that fibers with a diameter smaller than 0.4 μm reflect slower oscillations and result in slower frequencies than the theta band. In addition, fibers larger than 3 μm in diameter could be involved in the faster frequency response than the 20–32 Hz band.

The posterior pole of the CC is effective in visual information transfer mainly between the occipital and parietal sites (Zeki 1993). In areas 17 and 18 of the cat visual cortex, Molotchnikoof et al. (1996) performed single unit recordings and found that an increasing number of cortical neurons showed oscillations in the frequency range of 22–102 Hz to visual stimuli. Engel et al. (1991) demonstrated that the response synchronization in the high-frequency range between cell groups in area 17 of the two hemispheres is abolished by severing the CC. Also, Munk et al. (1995) reported that sectioning of the CC between areas 17 and 18 in cats led to an abolition of interhemispheric synchronization in the beta and gamma bands. Knyazeva et al. (1999) analyzed the coherence of EEG signals recorded symmetrically from the two hemispheres while subjects were viewing visual stimuli. They found that visual stimuli cause interhemispheric synchronization, particularly at 25–45 Hz. These findings suggested that callosal connections are necessary for the synchronous, stimulus-induced activity of visual areas in the two hemispheres, which is thought to play a role in the “binding” process (Singer 1993). The method used in our study seems to be sensitive to the fast interhemispheric transfer in fibers around 3 μm in diameter, which oscillate in the beta2 band, but not sensitive enough to capture the largest fibers around 5 μm in diameter, which oscillate with higher frequencies than 32 Hz.

The percentages of fibers with different diameters only in the posterior pole of the CC are given in Table 3. These values were calculated considering the data provided by Aboitiz et al. (1992). The portion of

Table 3. Percentages of fibers larger than 0.4 μm in diameter in posterior pole of CC according to Aboitiz et al. (1992)

Fiber diameter (μm)	Posterior pole fiber (%)
0.4–1	74–77
1–3	23–25
3–5	< 0.1
> 5	< 0.05

callosal fibers between 0.4 and 1.0 μm in diameter is 74% and 77% of the total number of myelinated fibers in the posterior part of the CC, which is most active for transfer of visual information. Table 4 sums up the energy percentages of theta and alpha bands given in Tables 1 and 2 separately for LVF and RVF and also sums up beta1 and beta2 bands similarly. The summation of energy percentages of IVEPs in theta and alpha is found to be between 76.2% and 81.6% (Table 4), which is close to the value 74–77% for fibers 0.4–1 μm in diameter obtained from the anatomical study of the human CC (Table 4). As also seen in Table 4, the sum of energy percentage in the beta1 and beta2 bands is between 18.4% and 24.2%, which probably reflects the proportion of activation of callosal fibers 1–3 μm in diameter.

According to our estimate of fiber proportion, results also indicate an asymmetry of callosal transfer. The proportion of slow fibers (0.4–1.0 μm in diameter) for LVF experiments is smaller than that for RVF experiments. The proportion of activated larger fibers (1–3 μm) in LVF experiments is larger than that for RVF experiments.

Asymmetric IHTT was first suggested by Marzi et al. (1991), who carried out meta-analysis on 16 simple RT studies. They found RT advantages for the LVF, indicating faster transfer from the right-to-left hemisphere than from the left-to-right. Meta-analysis of VEP-IHTT by Brown et al. (1994) supported this report of Marzi et al. (1991), indicating the similar directionally asymmetric transmission. Of 18 independent measures of N160-IHTT from the occipital region, 12 showed clear asymmetries, which was consistent with faster IHTT from right to left, 3 studies showed no asymmetry, and the remaining 3 showed an asymmetry in the opposite direction. In our study, besides a greater proportion of larger-dimension fibers, we also found relatively shorter delays in LVF experiments compared to RVF experiments. This supported the previous findings concerning asymmetric callosal transfer, indicating faster transfer from the right hemisphere to the left.

This study depends on the assumption that each fiber of the CC creates the same potential at the opposite hemisphere irrespective of the fiber dimension. However, fine anatomical studies showed that there are remarkable differences for fine radial and tangential distributions of individual callosal axons (Innocenti et al. 1995;

Table 4. Summation of energy percentages of IVEPs in the theta–alpha band and beta1–beta2 band. Stimuli were applied to RVF or LVF at the occipital or parietal site

Recording site	Left or right visual field experiments	Theta–alpha (5–15 Hz) Fibers 0.4–1 μm in diameter (%)	Beta1–Beta2 (15–32 Hz) Fibers 1–3 μm in diameter (%)
Occipital	LVF	76.2	24.2
	RVF	80.4	20.1
Parietal	LVF	77.8	22.6
	RVF	81.6	18.4

Hauzel and Milleret 1999). The formulation used in this study required some correction coefficients considering individual features of callosal fibers. However, to our knowledge, fine anatomical data of the brain that show a distribution of terminal axons of callosal fibers in different dimension have not been reported until now.

More experiments are needed for more reliable results. However, this study gives us an idea on how to use time-frequency analysis and cross correlation of signals in the determination of IHTT. Using frequency-dependent shifts in time and maximizing the cross correlation of DVEP-IVEP pairs in the time-frequency domain, we would be able to examine the delay not only at P100 and N160 peaks but along a meaningful time interval as well. Furthermore, by shifting forward the directly stimulated VEP according to the delay estimated at each time window, the amplitudes and also energies of the synchronized DVEP-IVEP pairs are compared at the chosen frequency bands. The percentages at each band should be examined further in conjunction with the distribution of axon diameters in the posterior pole of the CC, questioning the relation between the distributions of the axon diameters and activations at each band.

According to our model, the negative correlation of magnitudes and energies with frequency bands is conclusive for IVEP signals. This is due to the ratio of callosal fibers of different diameters, which depends on the speed of transmitted frequency. However, the same correlation was obtained for DVEP signals derived from the contralateral hemisphere. How can we explain this negative correlation for the DVEP signals without using the callosal model? DVEP reflects the results of parallel processing in visual pathways from the retina to the LGN and from the LGN to the primary visual cortex. It is widely known that these parallel visual pathways have different information channels relating to different aspects of retinal image such as color, form, and movement: the neurons of magnocellular pathways have larger axons and high firing aspects because these neurons process movement with higher temporal resolution. On the other hand, the neurons of parvocellular pathways have relatively smaller axons and slower firing rates, but there is a large amount of neurons in comparison with magnocellular system, relating to high spatial resolution (Kandel et al. 2000). DVEP is the response of contralateral visual cortical areas to stimuli, and the response contains different aspects of visual stimuli that transfer through parallel and physically different information channels. Therefore, this visual information would be transferred to the ipsilateral cortical areas via callosal fibers that show similar aspects like visual pathways from retina to cortex. Otherwise, aspects of visual-sensorial and perceptual process could not be transferred from one hemisphere to the other.

This approach gives us an opportunity to learn more about the nature of hemispheric integration and individual differences, including the role of the CC in certain clinical disorders. The CC is known to be involved in many developmental brain disorders including schizophrenia (David 1994; and Endrass et al. 2002), dyslexia (Saron and Davidson 1989), attention deficit hyperac-

tivity disorder (Giedd et al. 1994), etc. A significant advantage can be gained by estimating the callosal fiber composition in normal and abnormal developmental processes in which a noninvasive electrophysiological method is used.

Finally, we believe that our approach contributes to the understanding of the nature of callosal transfer. In addition, it gives us not only a model for understanding the interhemispheric transfer but also a model for understanding all information transfer between two distinct regions in the neural system.

References

- Aboitiz F, Scheibel AB, Fisher RS, Zaidel E (1992) Fiber composition of the human corpus callosum. *Brain Res* 598: 143–153
- Bashore TR (1981) Vocal and manual reaction time estimates of inter-hemispheric transmission time. *Psychol Bull* 89: 352–368
- Başar E (1988) EEG-dynamics and evoked potentials in sensory and cognitive processing by the brain. In: Başar E (ed) *Dynamics of sensory and cognitive processing by the brain*. Springer, Berlin Heidelberg New York, pp 30–55
- Brown WS, Jeeves MA (1993) Bilateral visual field processing and evoked potential inter-hemispheric transmission time. *Neuropsychologia* 31: 1267–1281
- Brown WS, Larson EB, Jeeves MA (1994) Directional asymmetries in inter-hemispheric transmission time: evidence from visual evoked potentials. *Neuropsychologia* 32: 439–448
- Clarke JM, Zaidel E (1994) Anatomical-behavioural relationships: corpus callosum morphometry and hemispheric specialization. *Behav Brain Res* 64: 185–202
- David AS (1994) Schizophrenia and the corpus callosum: developmental, structural and functional relationships. *Behav Brain Res* 64: 203–211
- Davidson RJ, Saron C (1992) Evoked potential measures of inter-hemispheric transfer time in reading disabled and normal boys. *Dev Neuropsychol* 22: 353–364
- Ducati A, Fava E, Motti EDF (1988) Neuronal generators of the visual evoked potentials: intracerebral recording in awake humans. *Electroencephalogr Clin Neurophysiol* 71: 89–99
- Endrass T, Mohr B, Rockstroh B (2002) Reduced inter-hemispheric transmission in schizophrenia patients: evidence from event-related potentials. *Neurosci Lett* 320: 57–60
- Engel AK, König P, Kreiter AK, Singer W (1991) Inter-hemispheric synchronization of oscillatory neuronal responses in cat visual cortex. *Science* 252: 1177–1179
- Gazzaniga MS (2000) Cerebral specialization and inter-hemispheric communication. *Brain* 123: 1293–1326
- Giedd JN, Castellanos FX, Casey BJ, Kozuch P, King AC, Hamburger SD, Rapoport JL (1994) Quantitative morphology of the corpus callosum in attention deficit hyperactivity disorder. *Am J Psychiatry* 151: 665–669
- Hauzel JC, Milleret C (1999) Visual inter-hemispheric processing: contrasting and potentialities set by axonal morphology. *J Physiol* 93: 271–284
- Hoptman MJ, Davidson RJ (1994) How and why do two cerebral hemispheres interact? *Psychol Bull* 116: 195–219
- Innocenti GM, Aggound-Zouaoui D, Lehman P (1995) Cellular aspects of callosal connections and their development. *Neuropsychologia* 33: 961–987
- Kandel ER, Schwartz JH, Jessell TM (2000) *Principles of neural science*. 4th edn. McGraw-Hill, New York, pp 501
- Knyazeva MG, Kiper DC, Vildavski VY, Despland PA, Meader-Ingvar M, Innocenti GM (1999) Visual stimulus-dependent changes in inter-hemispheric EEG coherence in humans. *J Neurophysiol* 82: 3095–3107

- Marzi CA, Bisiacchi P, Nicoletti R (1991) Is inter-hemispheric transfer of visuomotor information asymmetric? A meta-analysis. *Neuropsychologia* 29: 1163–1177
- Molotchnikoff S, Shumikhina S, Moisan LE (1996) Stimulus-dependent oscillations in the cat visual cortex: differences between bar and gratings stimuli. *Brain Res* 731: 91–100
- Munk MHJ, Nowak LG, Nelson JJ, Bullier J (1995) Structural basis of cortical synchronisation. II. Effects of cortical lesions. *J Neurophysiol* 74: 2401–2414
- Nalçacı E, Basar-Eroğlu C, Stadler M (1999a) Visual evoked potential inter-hemispheric transfer time in different frequency bands. *Clin Neurophysiol* 110: 71–81
- Nalçacı E, Basar-Eroğlu C, Stadler M (1999b) VEP-inter-hemispheric transfer time in 20–32 Hz band in man. *Neuroreport* 10: 3105–3109
- Nowak LG, Bullier J (1997) The timing of information transfer in the visual system. In: Rockland K, Kaas JH, Peters A (eds) *Cerebral cortex, extrastriate cortex in primates*, vol 12. Plenum, New York, pp 205–241
- Rugg MD, Lines CR, Milner AD (1984) Visual evoked potentials to lateralized stimuli and the measurement of inter-hemispheric transmission time. *Neuropsychologia* 22: 215–225
- Saron CD, Davidson RJ (1989) Visual evoked potentials measures of inter-hemispheric transfer time in humans. *Behav Neurosci* 103: 1115–1138
- Singer W (1993) Synchronization of cortical activity and its putative role in information processing and learning. *Annu Rev Physiol* 55: 349–374
- Swadlow HA (1974) Systematic variations in the conduction velocity of slowly conducting axons in the rabbit corpus callosum. *Exp Neurol* 43: 445–451
- Waxman SG, Bennett MVL (1972) Relative conduction velocities of small myelinated and non-myelinated fibers in the central nervous system. *Nature* 238: 217–219
- Zeki S (1993) *A vision of the brain*. Blackwell, Oxford, p 169